Effects of Intrinsic Flexibility on Adsorption Properties of Metal–Organic Frameworks at Dilute and Nondilute Loadings
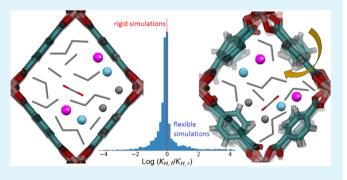
Mayank Agrawal and David S. Sholl*

School of Chemical and Biomolecular Engineering, Georgia Institute of Technology, Atlanta, Georgia 30332, United States

S *Supporting Information*

ABSTRACT: Molecular simulation of adsorption in nanoporous materials has become a valuable complement to experimental studies of these materials. In almost all cases, these simulations treat the adsorbing material as rigid. We use molecular simulations to examine the validity of this approximation for the adsorption in metal–organic frameworks (MOFs) that have framework flexibility without change in their unit cells because of thermal vibrations. All nanoporous materials are subject to this kind of framework flexibility. We examine the adsorption of nine molecules (CO_2, CH_4, ethane, ethene, propane, propene, butane, Xe, and Kr) and four molecular mixtures (CO_2/CH_4, ethane/ethene, propane/propene/butane, and Xe/Kr) in 100 MOFs at dilute and nondilute adsorption conditions. Our results show that single-component adsorption uptakes at nondilute conditions are only weakly affected by framework flexibility, but adsorption selectivities at both dilute and nondilute conditions can be significantly affected by flexibility. The most dramatic impacts of framework flexibility occur for adsorption uptake in the limit of dilute adsorption. These results suggest that the importance of including framework flexibility when attempting to make quantitative predictions of adsorption selectivity in MOFs and similar materials may have been underestimated in the past.

KEYWORDS: metal–organic frameworks, flexibility, Monte Carlo, molecular dynamics, adsorption, separation

INTRODUCTION

Metal–organic frameworks (MOFs) have attained significant attention in the scientific community because of their diverse applications in gas storage, separations, catalysis, sensing, and drug delivery. MOFs have highly tunable chemical and geometrical properties, high surface areas, and a wide range of pore sizes. One interesting aspect of MOFs is the flexibility of the frameworks that can be responsive to external stimuli such as adsorption of guests, temperature, pressure, light irradiation, and mechanical forces.[1−5] Structural flexibility in MOFs can be divided into two classes: variations resulting in changes in the unit cell volume and changes that occur without variation in the unit cell volume, V. Flexibility with $\Delta V \neq 0$, which includes breathing, swelling, and subnetwork displacement, has been extensively studied.[6,7] It is important to note, however, a material that goes through significant variations in volume may cause significant operational complications in many practical applications. It is therefore not clear from an applied point of view whether the subset of MOFs with these properties is desirable. Flexibility that occurs with $\Delta V = 0$ includes effects such as thermal vibrations and linker rotation.[5,6,8−10] This second kind of flexibility occurs in all MOFs. It is therefore interesting to understand how modes of flexibility with $\Delta V = 0$ affect the properties of MOFs.
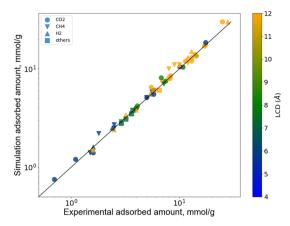
Molecular simulations have become a useful tool for predicting the adsorption properties of molecules in diverse collection of MOFs and similar materials. These simulations have been used to predict the adsorption properties of a diverse range of molecules in large libraries of MOF structures.[11−18] In almost all molecular simulations of adsorption in MOFs to date, the MOF structure is assumed to be rigid. This assumption is made for reasons of both computational efficiency and convenience; performing simulations with flexible MOFs is far more computationally intensive and also requires specification of more complex force fields (FFs). Even in simulations that examine adsorption in MOFs with breathing modes and related phenomena, a typical approach is to perform simulations for a range of distinct rigid crystal structures and then to combine these results using appropriate thermodynamic criteria.[19,20]

One common justification for approximating MOFs as rigid during simulations of adsorption is that predictions from this approach are often consistent with experiments. We illustrate this point in Figure 1 with data from rigid structure calculations from 24 studies on 20 different MOFs and nine different molecules.[21−43] Details of all data points and the FFs used in each simulation are given in Table S1. Most of these simulations used generic FFs such as the Universal Force Field

Figure 1. Comparison of adsorption uptake of various adsorbates in a range of MOFs between experiments and GCMC simulated values using rigid crystal structures (● = CO_2, ▼ = CH_4, ▲ = H_2, and ■ = other adsorbates) from the previous literature. Details of all data points are given in the Supporting Information.

(UFF),[44] DREIDING,[45] TraPPE,[46] and OPLS.[47] Simulation results that were obtained by directly fitting the underlying FF to the experiments used for comparison were excluded from this data set. There are, however, simulation data points in Figure 1 that were scaled by the authors of the simulation studies based on the difference in the experimental and theoretical surface area. Park et al.[48] compared experimental results with simulations using "standard" FFs and rigid crystal structures for CO_2 adsorption for all MOFs for which more than three independent experimental isotherms are available. They found that the simulation results for almost all of the materials overlap with the experimental data when a 15% relative error is allowed.

Despite the apparent success of modeling adsorption in MOFs using rigid structures, there are several studies that suggest that the flexibility with $\Delta V = 0$ in MOFs can significantly affect adsorption. Gee and Sholl.[10] used the so-called "flexible snapshots" method to show that constant volume flexibility in MIL-47 significantly affects the adsorption selectivity of C_8 aromatic isomers. This work found that the inclusion of framework flexibility in molecular simulations decreased the selectivity of o-xylene to ethylbenzene by an order of magnitude relative to simulations using rigid structures. The lower selectivity predicted by the more detailed calculations was in reasonable agreement with experimental observations. In a recent study, Witman et al.[12] studied the effect of flexibility on Xe/Kr selectivity in ∼3000 MOFs using a model that predicts a material's Henry regime adsorption and selectivity as a function of flexibility. The results obtained from this model were compared with molecular simulations at dilute loadings using the flexible snapshots method at 298 K. Witman et al. concluded that the selectivity of the Xe/Kr mixture can increase or decrease by up to two orders of magnitude because of inclusion of $\Delta V = 0$ framework flexibility.

These two papers raise the possibility that in some situations including framework flexibility in MOFs is necessary to achieve a quantitative description of adsorption in these materials. A limitation of the work by Witman et al.[12] is that it only considered adsorption at dilute loadings and that the analytical model introduced by the authors only applied to spherical molecules. It is conceivable that the impact of MOF flexibility on adsorption is most pronounced at dilute loadings, but it is

not possible to test this hypothesis with data already available in the literature. This observation motivated us to use molecular simulations to systematically study the impact of $\Delta V = 0$ flexibility of MOFs on adsorption properties for a range of molecular mixtures at dilute and nondilute loadings. To do so, we simulated the adsorption properties of four mixtures (CO_2/CH_4, ethane/ethene, propane/propene/butane, and Xe/Kr) at dilute and finite loadings in a set of 100 MOFs randomly chosen from CoRE MOF database.[49] Our simulations demonstrate that the flexibility can either increase or decrease selectivity for all mixtures for a given material at both dilute and finite loadings. Results obtained for Xe/Kr mixtures at dilute loadings are in good agreement with the work of Witman et al.[12] We quantitatively compare the effect of a framework's flexibility on selectivity depending on the material's pore size and adsorbate's diameter and find that molecules with kinetic diameters comparable to the adsorbing material's pore size are affected the most by framework flexibility. This observation is consistent at both dilute and finite loadings. Further, we demonstrate that there is no clear correlation for the dependence of selectivity on framework flexibility between dilute loadings and finite loadings. This suggests that understanding the overall impact of framework flexibility on adsorption in MOFs cannot be achieved in a simple way from simulations at dilute loadings.

Simulation Methods. For our calculations, 100 MOF structures were randomly chosen from a subset of the CoRE MOF database[49] consisting of >2900 different crystal structures for which high-quality atomic point charges have been reported.[50] The refcodes for these 100 structures are listed in Table S3, along with information on the largest cavity diameter (LCD), pore limiting diameter (PLD), and Brunauer−Emmett−Teller surface area of each structure. All structures in the CoRE MOF database are derived from experimentally reported crystal structures assuming that all the free solvent was removed from the crystal. Our simulations used FF-based Monte Carlo (MC) simulations as implemented in RASPA[51] to calculate adsorption properties of nine different compounds that are divided into four different mixtures, CO_2/CH_4, ethane/ethene, propane/propene/butane, and Xe/Kr. We studied the adsorption of each adsorbate at nondilute conditions and each mixture at dilute and nondilute conditions at room temperature.

Henry constants, K_H, were computed with the Widom insertion method.[52] These calculations also gave the helium void fraction and heat of adsorption (E_{ads}) in the limit of zero loading. We used equilibration and production periods of 1×10^5 MC cycles; preliminary tests indicated that this was sufficient to get well-converged results. To study adsorption at nondilute conditions, grand canonical MC (GCMC) simulations were performed using equilibrium and production periods of 5×10^5 MC cycles. Each MC cycle consisted of a trial insertion, deletion, reinsertion, translation, or rotation with equal probability. Our multicomponent GCMC simulations also included an additional MC move for exchanging adsorbed molecules to improve convergence. For nondilute simulations, the composition of all mixtures was taken to be equimolar in the bulk phase and external pressures were chosen to give moderate to high loadings. Multicomponent simulations were performed for CO_2/CH_4 and ethane/ethene mixtures at a total pressure of 20 bar, for Xe/Kr mixtures at 40 bar, and for propane/propene/butane mixtures at 10 bar.
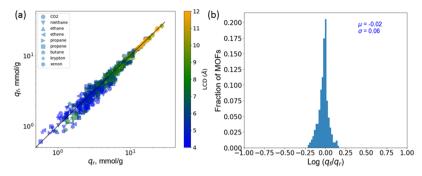
Figure 2. (a) Parity plot of single-component adsorbed amounts, (b) histogram of the ratio of single-component adsorbed amounts, using rigid (q_r) and flexible (q_f) simulations, for nine adsorbates in 100 MOFs at high pressures (CO_2, CH_4, ethane, and ethene: 20 bar each, Xe and Kr: 40 bar each, propane, propene, and butane: 10 bar each). The data points in the plot (a) are color-coded based on the LCD of each MOF.

The adsorption selectivity of a mixture at dilute loading is defined without approximation as the ratio of the single component Henry constants,[53] while the adsorption selectivity of a mixture at finite loading is defined by

$$\alpha_i = \frac{q_i}{\sum_{j,\, j \neq i} q_j} \times \frac{\sum_{j,\, j \neq i} p_j}{p_i} \tag{1}$$

where α_i is the selectivity of the ith component relative to all other components in the mixture, q_i is the loading of ith component, and p_i is the external partial pressure of the ith component.

Adsorbate−adsorbate interactions were defined using the TraPPE FF.[46] Adsorbate−MOF interactions were defined using Lorentz−Berthelot mixing rules with Lennard-Jones parameters taken from UFF[44] for the framework and the TraPPE[46] for the adsorbates. Coulombic interactions were computed using the Ewald method with a precision of 10^{-6} and a 13 Å cutoff. Point charges of atoms in MOFs were previously assigned using the DDEC method[50,54] and point charges on atoms in adsorbates were taken from TraPPE.[46] LJ potentials were truncated at a spherical cutoff distance of 13 Å.

All MOF degrees of freedom were described using the modified universal FF introduced by Coupry et al. for MOFs known as UFF4MOF.[55] For calculations using rigid structures, we first relaxed the MOF structure reported by the CoRE MOF database using classical FFs in the LAMMPS package[56] and then fixed the atoms in the relaxed structure while performing MC simulations. To probe the effect of framework flexibility on adsorption, we used the flexible snapshot method developed by Gee and Sholl.[10] In this approach, an ensemble of empty MOF structures is generated by simulating the dynamics of the MOF. GCMC simulations are then performed independently for each structure in the ensemble. This approach is similar to what was used by Witman et al. to study the effect of flexibility on Xe/Kr selectivity at dilute loadings.[12] This method includes effects associated with $\Delta V = 0$ flexibility in the MOFs (e.g., variations in MOF coordinates because of thermal fluctuations), but it cannot give information on possible aspects of MOF flexibility that arise because of coupling with adsorbate degrees of freedom. We performed *NVT* MD simulations after structure relaxation using LAMMPS at 300 K to account for the flexibility without volume change in the selected MOFs. The temperature in these simulations was controlled using the Nosé−Hoover thermostat with a decay period of 0.1 ps. MD simulations were performed with a time step of 1.0 fs for an equilibration period

of 500 ps and production period of 1 ns. The computational expense of the flexible snapshot method is determined by the number of distinct snapshots used because an independent GCMC simulation must be performed for every snapshot. It is therefore important to select snapshots from structures that are uncorrelated. To this end, snapshots from our MD simulations were taken every 100 ps from the production period for a total of 10 snapshots. Adsorption properties of flexible materials were described using data averaged over these 10 snapshots. It is also possible to generate MOF snapshots using ab initio MD, which has the advantage of not requiring a FF, but this approach is far more computationally intensive.[57,58]

■ RESULTS AND DISCUSSION

Effects of Flexibility in MOFs on Single-Component Adsorption at Nondilute Loadings. We first consider single component adsorption in MOFs at high pressures. As shown in Figure 1, previous literature suggests that simulations using rigid structures are often able to predict single-component adsorption in MOFs. To explicitly test the role of the rigid structure approximation, we performed single-component adsorption calculations for CO_2, CH_4, ethane, ethene, propane, propene, butane, Xe, and Kr at 20, 20, 20, 20, 10, 10, 10, 40, and 40 bar, respectively. These pressures were chosen to give moderate to high loadings at 298 K. The rigid and flexible single component adsorption uptakes (q_r and q_f) of these nine adsorbates in 100 MOFs and a histogram of their ratio are shown in Figure 2. Although including flexibility can influence the adsorption uptake, this effect is not strong. All of the examples we considered show a difference of less than 30% between the rigid and flexible calculations, and the average absolute error between the two sets of calculations is 6.2%. The impact of flexibility is reduced in MOFs with large pores; the average absolute error for MOFs with LCD < 6 Å (LCD > 6 Å) is 9% (5%).

It is important to consider whether these results are consistent with the studies discussed above that showed strong effects because of including framework flexibility.[10,12] The work of Gee and Sholl[10] and Witman et al.[12] examined different adsorption properties than the high-pressure single-component results shown in Figure 2. This hints that different kinds of adsorption properties can have different sensitivity to framework flexibility. An example is the work of Gee and Sholl,[43] which showed that calculations using rigid structure approximation gave useful results for single-component adsorption isotherms of C_8 aromatics in MIL-47 but that simulations with the same FFs do not accurately predict the
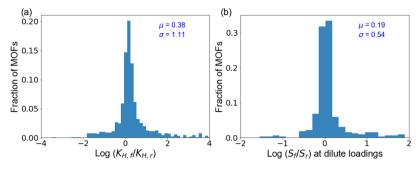
Figure 3. Histogram of the ratio of room temperature (a) Henry constants of nine adsorbates and (b) selectivity of four mixtures in 100 MOFs calculated using flexible and rigid simulations. Mean μ and standard deviation σ are shown for each data set.
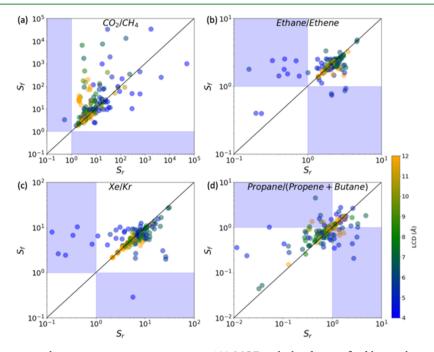

Figure 4. Dilute loading mixture selectivities at room temperature in 100 MOFs calculated using flexible simulations (vertical axes) and rigid simulations (horizontal axes) for (a) CO_2/CH_4, (b) ethane/ethene, (c) Xe/Kr, and (d) propane/propene/butane. The data points are color-coded based on the LCD of each MOF.

selectivity of C_8 aromatic mixtures.[10] To examine this issue further, we studied the effect of flexibility on Henry constants (i.e., adsorption at dilute loadings) and mixture selectivity at both dilute and nondilute loadings.

Effect of Flexibility in MOFs on Adsorption Properties at Dilute Loadings. At the limit of dilute adsorption, the Henry's constant characterizes adsorption affinity for both pure components and adsorbed mixtures. We calculated the Henry's constants of all nine adsorbates in the 100 MOFs listed in Table S3 using both flexible ($K_{H,f}$) and rigid simulations ($K_{H,r}$). Figure 3a shows the ratios of the resulting Henry constants. If adsorption in a MOF was completely unaffected by flexibility, the logarithmic ratio shown in Figure 3a would be zero. Figure 3a shows, however, that framework flexibility can change the Henry's constants by as much as 2 orders of magnitude. Out of 900 data points in the histogram, 319 MOF−adsorbate pairs have $|\log(K_{H,f}/K_{H,r})| < 0.1$, which means that change in Henry constants due to flexibility is less than ∼25%. 413 pairs have $0.1 < |\log(K_{H,f}/K_{H,r})| < 1$, meaning the change in Henry constants due to flexibility is between a factor of 1.25 and 10, and 72 pairs have $1 < |\log(K_{H,f}/K_{H,r})| < 2$. There are 42 MOF−adsorbate pairs for which $|\log(K_{H,f}/K_{H,r})| > 4$, representing

cases where flexibility has an enormous effect on adsorption. In most of these extreme cases, the MOFs have pore sizes very similar to the adsorbing molecule's diameter. Figure S1 shows the histogram of the ratio of $K_{H,f}$ and $K_{H,r}$ for each adsorbate with the standard deviations individually. Figure S1 shows that the standard deviations are consistently higher for the larger molecules among the nine adsorbates, indicating that flexibility typically has more significant effects on larger molecules.

Figure 3a makes it clear that in at least a fraction of MOFs, framework flexibility strongly influences adsorption of individual molecules at dilute loadings. However, it might be expected (or perhaps hoped) that these effects might partially cancel when the separation of a mixture is studied if the changes in K_H among different adsorbates are correlated. Figure 3b shows the impact of framework flexibility at dilute loading on the selectivity of CO_2/CH_4, ethane/ethene, propane/propene/butane, and Xe/Kr mixtures in each MOF. Although the impact of flexibility on selectivity is often less than that for the individual adsorbed amounts, there are still plentiful examples where the effect is not negligible. Thirty percentage of the MOF−adsorbate pairs show a change in Henry constants less than 25% because of flexibility, but almost

45% of the MOF−mixture pairs that show a similar low change in selectivity. The Henry's constants in 46% of the MOF−adsorbate pairs changed by more than a factor of 2 ($|\log(K_{H,f}/K_{H,r})| > 0.3$) while the selectivity in 36% of the MOF−mixture pairs changed by more than the same factor. We examine this situation in more detail in Figure 4 by showing the impact of flexibility on mixture selectivity for the four different mixtures. The regions shaded in light blue in Figure 4 indicate cases where the rigid and flexible simulations make qualitatively different predictions for which the molecule in the mixture is favorably adsorbed. This occurs more commonly in examples where the overall selectivities are moderate (e.g., ethane/ethene) than when typical selectivities are higher (e.g., CO_2/CH_4). For CO_2/CH_4 mixtures, selectivities as high as 10^4 are predicted and the effect of flexibility gets stronger (on average) as the selectivity increases.

Figures 2 and 4 hint that the MOFs whose properties are most strongly affected by their flexibility have diameters below 6 Å. To probe this further, we show the ratios of Henry's constants as a function of Δd, the difference between the adsorbate's kinetic diameter and the MOF's in Figure 5. The
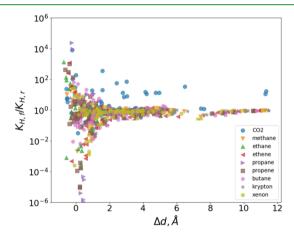

Figure 5. Ratio of Henry's constants ($K_{H,f}/K_{H,r}$) in simulations with flexible and rigid MOFs as a function of Δd, the difference between the MOF's LCD and the adsorbate's kinetic diameter.

kinetic diameter of a molecule is not a rigorously defined quantity, but it is a useful proxy for the molecular size (see Table S2). In MOFs whose cavities are much larger than the adsorbing molecule, the effects of flexibility on adsorption are typically small except for CO_2, which may be associated with the observation that this is the only nonpolar molecule we simulated. To further explore this issue, we calculated the Henry constants of CO_2 while turning off electrostatic interactions of the molecule with the framework and found that these (unphysical) nonpolar CO_2 molecules show behavior consistent with other nonpolar molecules (see Figure S2). These observations indicate that flexibility can have significant effects even for some MOFs that have much larger LCDs than the adsorbate's kinetic diameter when electrostatic interactions are important. Figure 5 has some data points for which $\Delta d < 0$, which might superficially suggest that molecules cannot adsorb at all. To avoid being misled by examples in which adsorption is negligible, we excluded from Figure 5 any examples for which the simulated adsorbed loading was less than 0.5 mmol/g at high pressures. Correlations between our simulated Henry constants with the MOF's LCDs and Δd are shown in Figures S3 and S4. We performed similar calculations

for heats of adsorption of all adsorbates and found that values of Henry constants and heats of adsorption are strongly correlated with each other calculated using both rigid and flexible calculations (see Figure S5). This observation is consistent with a previous study on adsorption properties of CWAs in MOFs[11] which indicates that flexibility effects on heat of adsorption would be similar to its effects on Henry constants. The effect of flexibility on the heats of adsorption is shown in Figures S6 and S7.

It is clear from the discussion above that flexibility in a MOF can significantly affect its adsorption properties at dilute loadings. MOFs that have LCDs comparable to the kinetic diameters of the adsorbates of interest have the largest effects of flexibility on their adsorption properties. These conclusions are entirely consistent with the previous work by Witman et al.[12] for Xe/Kr mixtures at dilute loadings.

Effects of Flexibility in MOFs on Multicomponent Adsorption at High Loadings. We now consider adsorption selectivity at nondilute loadings. For nondilute loadings, we performed multicomponent GCMC simulations to obtain adsorption selectivities for each mixture. In these calculations, all bulk mixtures are equimolar and pressures were chosen to give moderate (although not necessarily saturated) pore loadings. Figure 6 shows the impact of flexibility on selectivity
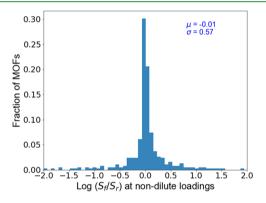

Figure 6. Histogram of the ratio of flexible and rigid room temperature selectivity at nondilute loadings of four mixtures of CO_2/CH_4 at P_{total} = 20 bar, ethane/ethene at P_{total} = 20 bar, Xe/Kr at P_{total} = 40 bar, and propane/(propene + butane) at P_{total} = 10 bar in 100 MOFs. Mean μ and standard deviation σ are shown for each data set.

at nondilute loadings. About 50% of the MOF−mixture pairs show a change in selectivity less than 25% because of flexibility at nondilute loadings, similar to the 45% of MOF−mixture pairs at dilute loadings. The selectivity in 27% of cases we considered changed by more than a factor of 2 ($|\log(S_f/S_r)| > 0.3$) at nondilute loadings, compared to 35% at dilute loadings. As with the results for dilute conditions, there are multiple examples at nondilute conditions for which the identity of the species that is selectively adsorbed is changed when flexibility is included (shown by the shaded regions in Figure S8). As for dilute loadings, MOFs that have LCDs comparable to the kinetic diameters of the adsorbates in the mixture are affected the most by flexibility (see Figure S9).

Comparison of the Effect of Flexibility in MOFs on Different Adsorption Properties. The standard deviations for the ratio of various adsorption properties in rigid and flexible MOFs are summarized in Table 1. Our results show that single-component adsorption uptakes in the dilute limit

Table 1. Standard Deviations of the Logarithmic Ratio of Adsorption Properties Using Flexible and Rigid Simulations for Henry's Constants, K_H, Adsorption Selectivities, S, and Adsorbed Amounts, q

	all MOFs	MOFs with LCD < 6 Å
$std(log10(K_{H,f}/K_{H,r}))$ at dilute loading	1.11	1.58
$std(log10(S_f/S_r))$ at dilute loading	0.54	0.69
$std(log10(S_f/S_r))$ at non-dilute loadings	0.57	0.71
$std(log10(q_f/q_r))$ non-dilute loadings	0.06	0.08

Figure 7. Ratio of room temperature flexible and rigid selectivities (S_f/S_r) at nondilute conditions and dilute conditions for 100 MOFs. Data points are color-coded according to the MOF's LCD.

(i.e., Henry's constants) are far more sensitive to the inclusion of framework flexibility than adsorption uptake at moderate and high loadings. Adsorption selectivity is more sensitive to the inclusion of flexibility than single-component loadings at nondilute conditions, but there is not a significant difference between the sensitivity of adsorption selectivities at dilute and nondilute conditions. Interestingly, these results imply that on average, the effects of framework flexibility tend to partially cancel out between different species at dilute conditions, but under nondilute conditions, adsorption selectivity is more strongly impacted by flexibility than by the individual loadings.

With the exception of the single-component loadings at nondilute conditions, all of the standard deviations listed in Table 1 correspond to effects that are large relative to usual thinking about the precision of computational predictions for adsorption in nanoporous materials. If these standard deviations are used to define an interval estimate, then a mixture selectivity for a flexible structure can be expected to lie within $[0.27S_r, 3.7S_r]$, where S_r is the result from a rigid material. This interval estimate is wider if attention is restricted to molecule/MOF pairs where the adsorbing molecule is similar in size to the MOF's pores. If experimental data were reported with uncertainties that are similar in range, it is not clear that such data would be viewed as useful. This observation suggests that the impact of framework flexibility on adsorption selectivity in nanoporous materials may have been underappreciated and may require more careful consideration in the future. The situation for understanding single-component adsorption is perhaps less dramatic. The interval estimate for q_f implied by Table 1 is $[0.87q_r, 1.15q_r]$.

From a computational point of view, simulations at dilute loading are much less demanding than simulations at nondilute loadings. This observation has been used by Tang et al. to develop methods that predict complete isotherms based solely on dilute loading simulations and textural information about the adsorbing material.[59] In our calculations, a similar percentage of MOF−adsorbate pairs show change in selectivity due to flexibility at dilute and nondilute conditions. An obvious question that emerges is whether it is possible to easily predict the effect of flexibility at nondilute loadings from simulations at dilute conditions. To answer this question, we compared the ratio of rigid and flexible mixture selectivities for both dilute and nondilute conditions in Figure 7. Although the variance in the relative impact of flexibility on selectivity is not significantly different between the two situations, there is not a clear correlation between the effect of flexibility at dilute loadings and nondilute loadings. More specifically, the Pearson product−moment correlation coefficient[60] is 0.66, 0.83, 0.93, and 0.75 for CO_2/CH_4, ethane/ethene, Kr/Xe, and propane/(propene + butane) mixtures, respectively. Further detail is provided for individual mixtures in Figure S10. The effect of
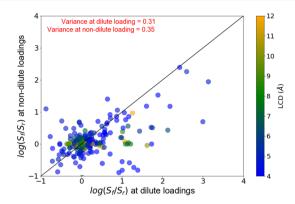
flexibility at dilute and nondilute conditions is the least correlated for CO_2/CH_4 mixtures and it is the most correlated for Kr/Xe mixtures (see Figure S10). This hints that the approximate model for spherical species at dilute loadings developed by Witman et al.[12] may be of limited applicability in predicting the sensitivity to flexibility in more complex adsorbed mixtures.

We have established that effects of flexibility on adsorption selectivity at dilute loadings and nondilute loadings are similar in magnitude but are not always correlated with each other. To better understand the impact of loading, we studied the effect of flexibility on selectivity of equimolar Xe/Kr and CO_2/CH_4 mixtures at different total pressures/loadings in the range of 1−40 bar. Figure S11 compares S_f/S_r at different pressures and shows that the mean and standard deviations at all pressures are similar for both mixtures. Figure 8 shows the Pearson product−moment correlation coefficients between S_f/S_r at different pressures for CO_2/CH_4 and Xe/Kr mixtures. For the CO_2/CH_4 mixture (Figure 8a), the correlation coefficients between S_f/S_r at different pressures are between 0.65 and 0.83, which indicates that even though the means and variances of S_f/S_r are similar, the results at one pressure are of limited value to predict the effect of flexibility at another pressure. As might be expected, the correlation coefficients are higher for the pressures that are closer to each other. For Xe/Kr mixtures (Figure 8b), the correlation coefficients at all conditions are above 0.9. This suggests that the mathematical model for spherical species at dilute loadings developed by Witman et al.[12] might be useful for predicting flexibility effects at nondilute conditions for this simple mixture.

■ SUMMARY

In this paper, we have used molecular simulations to probe the role of framework vibrations on the adsorption properties of MOFs. The effects we examined are relevant to all MOFs, an observation emphasized by our choice to study only flexibility associated with no volume change. The sizeable literature on modeling molecular adsorption in MOFs almost uniformly assumes that these flexibility effects can be neglected, an assumption which, if accurate, greatly improves the numerical efficiency of simulating adsorption. We used a "flexible snapshot" approach in which adsorption in multiple realizations of a flexible MOF are separately simulated as rigid structures. This approach is computationally efficient, but it does not account for effects because of deformation or flexibility of the MOF induced by adsorbed species. It seems
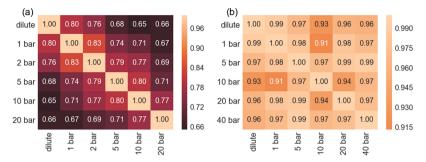
Figure 8. Correlation coefficients between S_f/S_r at different loading conditions for (a) CO_2/CH_4, (b) Xe/Kr mixtures. Both mixtures are equimolar, and x and y axis in the plot show the total pressure.

plausible, however, that if the effects of flexibility detected by this method are small, then the impact of further adsorbate–MOF coupling is also small in many cases. We presented results for multiple adsorbing molecules and adsorbing mixtures in 100 MOFs at both dilute and nondilute loadings, allowing us to systematically examine several distinct regimes.

A key outcome from our calculations is that the importance of framework flexibility on adsorption in MOFs varies considerably depending on the specific aspect of adsorption of interest. For single-component adsorption, the impact of flexibility is much more pronounced in the dilute adsorption limit (i.e., for Henry's constants), than it is at nondilute loadings. In mixture adsorption, the selectivity of adsorption is more sensitive to flexibility than the uptake of individual components, an observation that holds at both dilute and nondilute loadings. These results are fully consistent with previous simulation studies that examined a much smaller range of situations.[10,12]

Our results show that MOFs that have pore sizes comparable to the kinetic diameters of adsorbing molecules are the most affected by framework flexibility. For MOFs that have LCDs less than 6 Å, flexibility affects the Henry constants of the molecules we considered by an average factor of 33. For the same MOFs, flexibility affects the selectivity at dilute and nondilute by an average factor of 3.5. About 5% of the examples that we considered, including flexibility, reversed the predicted selectivity for mixtures. Moreover, we found that the effect of flexibility at dilute loadings does not correlate in a simple way with the effects at nondilute loadings.

Overall, our results indicate that appropriate consideration of framework flexibility may be important in any effort to make quantitative predictions about molecular adsorption in MOFs. The snapshot-based approach we have used provides a relatively straightforward means to estimate these effects, albeit one that is 5−10 times more computationally expensive than standard simulation methods based on rigid crystal structures.

ASSOCIATED CONTENT

ⓢ Supporting Information

The Supporting Information is available free of charge on the ACS Publications website at DOI: 10.1021/acsami.9b10622.

Kinetic diameters of the molecules; refcodes of 100 MOFs studied with their LCDs, PLDs, and surface areas; supporting figures for dilute and nondilute adsorption properties (PDF)

Simulation data used to plot all the figures (ZIP)

LAMMPS input data files to run MD calculations for MOFs (ZIP)

AUTHOR INFORMATION

Corresponding Author

*E-mail: david.sholl@chbe.gatech.edu.

ORCID ⓘ

David S. Sholl: 0000-0002-2771-9168

Notes

The authors declare no competing financial interest.

REFERENCES

(1) Férey, G.; Serre, C. Large Breathing Effects in Three-Dimensional Porous Hybrid Matter: Facts, Analyses, Rules and Consequences. *Chem. Soc. Rev.* **2009**, *38*, 1380−1399.

(2) Serre, C.; Millange, F.; Thouvenot, C.; Noguès, M.; Marsolier, G.; Louër, D.; Férey, G. Very Large Breathing Effect in the First Nanoporous Chromium(III)-Based Solids: MIL-53 or Cr^{III} (OH)· $\{O_2C−C_6H_4−CO_2\}·\{HO_2C−C_6H_4−CO_2H\}x ·H_2O_Y$. *J. Am. Chem. Soc.* **2002**, *124*, 13519−13526.

(3) Agrawal, M.; Bhattacharyya, S.; Huang, Y.; Jayachandrababu, K. C.; Murdock, C. R.; Bentley, J. A.; Rivas-Cardona, A.; Mertens, M. M.; Walton, K. S.; Sholl, D. S.; Nair, S. Liquid-Phase Multicomponent Adsorption and Separation of Xylene Mixtures by Flexible MIL-53 Adsorbents. *J. Phys. Chem. C* **2018**, *122*, 386−397.

(4) Kitaura, R.; Fujimoto, K.; Noro, S.-i.; Kondo, M.; Kitagawa, S. A Pillared-Layer Coordination Polymer Network Displaying Hysteretic Sorption: $[Cu_2(Pzdc)_2(Dpyg)]_n$(Pzdc= Pyrazine-2,3-Dicarboxylate; Dpyg = 1,2-Di(4-Pyridyl)Glycol). *Angew. Chem., Int. Ed.* **2002**, *41*, 133−135.

(5) Schneemann, A.; Bon, V.; Schwedler, I.; Senkovska, I.; Kaskel, S.; Fischer, R. A. Flexible Metal-Organic Frameworks. *Chem. Soc. Rev.* **2014**, *43*, 6062−6096.

(6) Zhang, J.-P.; Zhou, H.-L.; Zhou, D.-D.; Liao, P.-Q.; Chen, X.-M. Controlling flexibility of metal-organic frameworks. *Natl. Sci. Rev.* **2018**, *5*, 907−919.

(7) Bon, V.; Kavoosi, N.; Senkovska, I.; Kaskel, S. Tolerance of Flexible MOFs toward Repeated Adsorption Stress. *ACS Appl. Mater. Interfaces* **2015**, *7*, 22292−22300.

(8) Jiao, Y.; Li, Z.; Ma, Y.; Zhou, G.; Wang, S.; Lu, G. The Studies on Gas Adsorption Properties of MIL-53 Series MOFs Materials. *AIP Adv.* **2017**, *7*, 085009.

(9) Triguero, C.; Coudert, F.-X.; Boutin, A.; Fuchs, A. H.; Neimark, A. V. Mechanism of Breathing Transitions in Metal-Organic Frameworks. *J. Phys. Chem. Lett.* **2011**, *2*, 2033−2037.

(10) Gee, J. A.; Sholl, D. S. Effect of Framework Flexibility on C_8 Aromatic Adsorption at High Loadings in Metal-Organic Frameworks. *J. Phys. Chem. C* **2016**, *120*, 370−376.

(11) Agrawal, M.; Sava Gallis, D. F.; Greathouse, J. A.; Sholl, D. S. How Useful Are Common Simulants of Chemical Warfare Agents at Predicting Adsorption Behavior? *J. Phys. Chem. C* **2018**, *122*, 26061−26069.

(12) Witman, M.; Ling, S.; Jawahery, S.; Boyd, P. G.; Haranczyk, M.; Slater, B.; Smit, B. The Influence of Intrinsic Framework Flexibility on Adsorption in Nanoporous Materials. *J. Am. Chem. Soc.* **2017**, *139*, 5547−5557.

(13) Li, S.; Chung, Y. G.; Snurr, R. Q. High-Throughput Screening of Metal-Organic Frameworks for CO_2 Capture in the Presence of Water. *Langmuir* **2016**, *32*, 10368−10376.

(14) Zhang, H.; Snurr, R. Q. Computational Study of Water Adsorption in the Hydrophobic Metal-Organic Framework ZIF-8: Adsorption Mechanism and Acceleration of the Simulations. *J. Phys. Chem. C* **2017**, *121*, 24000−24010.

(15) Altintas, C.; Avci, G.; Daglar, H.; Nemati Vesali Azar, A.; Velioglu, S.; Erucar, I.; Keskin, S.; Keskin, S. Database for CO_2 Separation Performances of MOFs Based on Computational Materials Screening. *ACS Appl. Mater. Interfaces* **2018**, *10*, 17257−17268.

(16) Brandt, P.; Nuhnen, A.; Lange, M.; Möllmer, J.; Weingart, O.; Janiak, C. Metal-Organic Frameworks with Potential Application for SO_2 Separation and Flue Gas Desulfurization. *ACS Appl. Mater. Interfaces* **2019**, *11*, 17350−17358.

(17) Avci, G.; Velioglu, S.; Keskin, S. High-Throughput Screening of MOF Adsorbents and Membranes for H_2 Purification and CO_2 Capture. *ACS Appl. Mater. Interfaces* **2018**, *10*, 33693−33706.

(18) Tarzia, A.; Takahashi, M.; Falcaro, P.; Thornton, A. W.; Doonan, C. J.; Huang, D. M. High-Throughput Screening of Metal-Organic Frameworks for Macroscale Heteroepitaxial Alignment. *ACS Appl. Mater. Interfaces* **2018**, *10*, 40938−40950.

(19) Coudert, F.-X. The Osmotic Framework Adsorbed Solution Theory: Predicting Mixture Coadsorption in Flexible Nanoporous Materials. *Phys. Chem. Chem. Phys.* **2010**, *12*, 10904−10913.

(20) Zhang, C.; Gee, J. A.; Sholl, D. S.; Lively, R. P. Crystal-Size-Dependent Structural Transitions in Nanoporous Crystals: Adsorption-Induced Transitions in ZIF-8. *J. Phys. Chem. C* **2014**, *118*, 20727−20733.

(21) Chen, Y.; Jiang, J. A Bio-Metal-Organic Framework for Highly Selective CO_2 Capture: A Molecular Simulation Study. *ChemSusChem* **2010**, *3*, 982−988.

(22) Ramsahye, N. A.; Maurin, G.; Bourrelly, S.; Llewellyn, P. L.; Devic, T.; Serre, C.; Loiseau, T.; Ferey, G. Adsorption of CO_2 in Metal Organic Frameworks of Different Metal Centres: Grand Canonical Monte Carlo Simulations Compared to Experiments. *Adsorption* **2007**, *13*, 461−467.

(23) Llewellyn, P. L.; Bourrelly, S.; Vagner, C.; Heymans, N.; Leclerc, H.; Ghoufi, A.; Bazin, P.; Vimont, A.; Daturi, M.; Devic, T.; Serre, C.; Weireld, G. D.; Maurin, G. Evaluation of MIL-47(V) for CO_2-Related Applications. *J. Phys. Chem. C* **2013**, *117*, 962−970.

(24) Cui, Y.-W.; Li, J.; Du, Z. F.; Peng, Y. Z. Cr(VI) Adsorption on Red Mud Modified by Lanthanum: Performance, Kinetics and Mechanisms. *PLoS One* **2016**, *11*, No. e0161780.

(25) Pérez-Pellitero, J.; Amrouche, H.; Siperstein, F. R.; Pirngruber, G.; Nieto-Draghi, C.; Chaplais, G.; Simon-Masseron, A.; Bazer-Bachi, D.; Peralta, D.; Bats, N. Adsorption of CO_2, CH_4, and N_2 on Zeolitic Imidazolate Frameworks: Experiments and Simulations. *Chem.—Eur. J.* **2010**, *16*, 1560−1571.

(26) Krishna, R.; van Baten, J. M. Investigating the Potential of MgMOF-74 Membranes for CO_2 Capture. *J. Membr. Sci.* **2011**, *377*, 249−260.

(27) Walton, K. S.; Millward, A. R.; Dubbeldam, D.; Frost, H.; Low, J. J.; Yaghi, O. M.; Snurr, R. Q. Understanding Inflections and Steps in Carbon Dioxide Adsorption Isotherms in Metal-Organic Frameworks. *J. Am. Chem. Soc.* **2008**, *130*, 406−407.

(28) Yang, Q.; Zhong, C. Molecular Simulation of Adsorption and Diffusion of Hydrogen in Metal−Organic Frameworks. *J. Phys. Chem. B* **2005**, *109*, 11862−11864.

(29) Greathouse, J. A.; Kinnibrugh, T. L.; Allendorf, M. D. Adsorption and Separation of Noble Gases by IRMOF-1: Grand Canonical Monte Carlo Simulations. *Ind. Eng. Chem. Res.* **2009**, *48*, 3425−3431.

(30) Farrusseng, D.; Daniel, C.; Gaudillère, C.; Ravon, U.; Schuurman, Y.; Mirodatos, C.; Dubbeldam, D.; Frost, H.; Snurr, R. Q. Heats of Adsorption for Seven Gases in Three Metal−Organic Frameworks: Systematic Comparison of Experiment and Simulation. *Langmuir* **2009**, *25*, 7383−7388.

(31) Zhuang, W.; Yuan, D.; Liu, D.; Zhong, C.; Li, J.-R.; Zhou, H.-C. Robust Metal-Organic Framework with an Octatopic Ligand for Gas Adsorption and Separation: Combined Characterization by Experiments and Molecular Simulation. *Chem. Mater.* **2012**, *24*, 18−25.

(32) Yang, Q.; Wiersum, A. D.; Jobic, H.; Guillerm, V.; Serre, C.; Llewellyn, P. L.; Maurin, G. Understanding the Thermodynamic and Kinetic Behavior of the CO_2/CH_4 Gas Mixture within the Porous Zirconium Terephthalate UiO-66(Zr): A Joint Experimental and Modeling Approach. *J. Phys. Chem. C* **2011**, *115*, 13768−13774.

(33) Hon Lau, C.; Babarao, R.; Hill, M. R. A Route to Drastic Increase of CO_2 Uptake in Zr Metal Organic Framework UiO-66. *Chem. Commun.* **2013**, *49*, 3634−3636.

(34) Granato, M. A.; Martins, V. D.; Ferreira, A. F. P.; Rodrigues, A. E. Adsorption of Xylene Isomers in MOF UiO-66 by Molecular Simulation. *Microporous Mesoporous Mater.* **2014**, *190*, 165−170.

(35) Borycz, J.; Lin, L.-C.; Bloch, E. D.; Kim, J.; Dzubak, A. L.; Maurice, R.; Semrouni, D.; Lee, K.; Smit, B.; Gagliardi, L. CO_2 Adsorption in Fe_2(Dobdc): A Classical Force Field Parameterized from Quantum Mechanical Calculations. *J. Phys. Chem. C* **2014**, *118*, 12230−12240.

(36) Zhang, Z.; Li, Z.; Li, J. Computational Study of Adsorption and Separation of CO_2, CH_4, and N_2 by an Rht-Type Metal-Organic Framework. *Langmuir* **2012**, *28*, 12122−12133.

(37) Peng, X.; Cheng, X.; Cao, D. Computer Simulations for the Adsorption and Separation of $CO_2/CH_4/H_2/N_2$ Gases by UMCM-1 and UMCM-2 Metal Organic Frameworks. *J. Mater. Chem.* **2011**, *21*, 11259−11270.

(38) Surblé, S.; Millange, F.; Serre, C.; Düren, T.; Latroche, M.; Bourrelly, S.; Llewellyn, P. L.; Férey, G. Synthesis of MIL-102, a Chromium Carboxylate Metal-Organic Framework, with Gas Sorption Analysis. *J. Am. Chem. Soc.* **2006**, *128*, 14889−14896.

(39) Garberoglio, G.; Skoulidas, A. I.; Johnson, J. K. Adsorption of Gases in Metal Organic Materials: Comparison of Simulations and Experiments. *J. Phys. Chem. B* **2005**, *109*, 13094−13103.

(40) Mileo, P. G. M.; Cavalcante, C. L.; Möllmer, J.; Lange, M.; Hofmann, J.; Lucena, S. M. P. Molecular Simulation of Natural Gas Storage in Cu-BTC Metal-Organic Framework. *Colloids Surf., A* **2014**, *462*, 194−201.

(41) Hamon, L.; Heymans, N.; Llewellyn, P. L.; Guillerm, V.; Ghoufi, A.; Vaesen, S.; Maurin, G.; Serre, C.; De Weireld, G.; Pirngruber, G. D. Separation of CO_2-CH_4 Mixtures in the Mesoporous MIL-100(Cr) MOF: Experimental and Modelling Approaches. *Dalton Trans.* **2012**, *41*, 4052−4059.

(42) Lucena, S. M. P.; Mileo, P. G. M.; Silvino, P. F. G.; Cavalcante, C. L. Unusual Adsorption Site Behavior in PCN-14 Metal-Organic Framework Predicted from Monte Carlo Simulation. *J. Am. Chem. Soc.* **2011**, *133*, 19282−19285.

(43) Gee, J. A.; Sholl, D. S. Prediction of Adsorption Properties of Cyclic Hydrocarbons in MOFs Using DFT-Derived Force Fields. *J. Phys. Chem. C* **2015**, *119*, 16920−16926.

(44) Rappé, A. K.; Casewit, C. J.; Colwell, K. S.; Goddard, W. A., III; Skiff, W. M. UFF, a Full Periodic Table Force Field for Molecular Mechanics and Molecular Dynamics Simulations. *J. Am. Chem. Soc.* **1992**, *114*, 10024−10035.

(45) Mayo, S. L.; Olafson, B. D.; Goddard, W. A. DREIDING: A Generic Force Field for Molecular Simulations. *J. Phys. Chem.* **1990**, *94*, 8897−8909.

(46) Martin, M. G.; Siepmann, J. I. Transferable Potentials for Phase Equilibria. 1. United-Atom Description of n-Alkanes. *J. Phys. Chem. B* **1998**, *102*, 2569−2577.

(47) Jorgensen, W. L.; Maxwell, D. S.; Tirado-Rives, J. Development and Testing of the OPLS All-Atom Force Field on Conformational Energetics and Properties of Organic Liquids. *J. Am. Chem. Soc.* **1996**, *118*, 11225−11236.

(48) Park, J.; Howe, J. D.; Sholl, D. S. How Reproducible Are Isotherm Measurements in Metal-Organic Frameworks? *Chem. Mater.* **2017**, *29*, 10487−10495.

(49) Chung, Y. G.; Camp, J.; Haranczyk, M.; Sikora, B. J.; Bury, W.; Krungleviciute, V.; Yildirim, T.; Farha, O. K.; Sholl, D. S.; Snurr, R. Q. Computation-Ready, Experimental Metal-Organic Frameworks: A Tool To Enable High-Throughput Screening of Nanoporous Crystals. *Chem. Mater.* **2014**, *26*, 6185−6192.

(50) Nazarian, D.; Camp, J. S.; Sholl, D. S. A Comprehensive Set of High-Quality Point Charges for Simulations of Metal-Organic Frameworks. *Chem. Mater.* **2016**, *28*, 785−793.

(51) Dubbeldam, D.; Calero, S.; Ellis, D. E.; Snurr, R. Q. RASPA: Molecular Simulation Software for Adsorption and Diffusion in Flexible Nanoporous Materials. *Mol. Simul.* **2015**, *42*, 81−101.

(52) Widom, B. Some Topics in the Theory of Fluids. *J. Chem. Phys.* **1963**, *39*, 2808−2812.

(53) Walton, K. S.; Sholl, D. S. Predicting Multicomponent Adsorption: 50 Years of the Ideal Adsorbed Solution Theory. *AIChE J.* **2015**, *61*, 2757−2762.

(54) Manz, T. A.; Limas, N. G. DDEC6: A Method for Computing Even-Tempered Net Atomic Charges in Periodic and Nonperiodic Materials. **2015**, arXiv:1512.08270v1.

(55) Coupry, D. E.; Addicoat, M. A.; Heine, T. Extension of the Universal Force Field for Metal-Organic Frameworks. *J. Chem. Theory Comput.* **2016**, *12*, 5215−5225.

(56) Plimpton, S. Fast Parallel Algorithms for Short-Range Molecular Dynamics. *J. Comput. Phys.* **1995**, *117*, 1−19.

(57) Watanabe, T.; Sholl, D. S. Accelerating Applications of Metal-Organic Frameworks for Gas Adsorption and Separation by Computational Screening of Materials. *Langmuir* **2012**, *28*, 14114−14128.

(58) Haldoupis, E.; Watanabe, T.; Nair, S.; Sholl, D. S. Quantifying Large Effects of Framework Flexibility on Diffusion in MOFs: CH_4 and CO_2 in ZIF-8. *ChemPhysChem* **2012**, *13*, 3449−3452.

(59) Tang, D.; Wu, Y.; Verploegh, R. J.; Sholl, D. S. Efficiently Exploring Adsorption Space to Identify Privileged Adsorbents for Chemical Separations of a Diverse Set of Molecules. *ChemSusChem* **2018**, *11*, 1567−1575.

(60) Cox, N. J. Speaking Stata: Correlation with Confidence, or Fisher's z revisited. *STATA J.* **2008**, *8*, 413−439.